DENDROBIOLOGY

2025, vol. 93, 42–59

https://doi.org/10.12657/denbio.093.003

*Ruiqiang Wang, Ke Liu, Yan Li, Tayeeba Tabussum Anni, Xuan Li, Binqiang Bao, Hongke Hao**

Stand spatial structure of Coniferous forests based on multi-source LiDAR data

Received: 2 December 2024; Accepted: 8 February 2025

Abstract: Coniferous forest spatial structure plays a critical role in forest management and ecological stability. However, traditional field survey methods for assessing stand spatial structure are labor-intensive, costly, and disruptive to ecosystems. To address these limitations, this study employs a multi-source LiDAR data fusion approach to explore intelligent methods for extracting stand spatial structure parameters.Using *Larix principis-rupprechtii Mayr* and *Picea wilsonii* as representative species, this study focuses on LiDAR data fusion as a core methodology to investigate intelligent approaches for extracting the spatial structure of forest stands in Shaanxi, China. The stand spatial structure parameters of the sample plot(including uniform angle index, neighborhood comparison and crowding degree) and the frequency were calculated and counted. The results showed that (1) in the coniferous forest stand with a total of 291 individual trees, the individual tree segmentation accuracy based on the integrated UAV-LiDAR and BLS data reached F = 0.96. (2) the Larix forest exhibited random distribution (R = 0.48), moderate size differentiation (U = 0.50), and average density (W = 0.75). The *Picea crassifolia* forest also showed random distribution (R = 0.48), moderate size differentiation (U = 0.47), and relatively high density (W = 0.94). The coniferous forest exhibited an unreasonable combination of tree distribution, with a frequency of 12%.The fused LiDAR data for parameter extraction and the calculation of forest stand spatial structure parameters enables faster and more effective analysis of spatial structure characteristics compared to traditional methods. Moreover, the multivariate distribution of these spatial parameters reveals internal structural features of the forest stand, allowing for the accurate identification of unreasonable structural combinations and providing a theoretical basis for optimizing and adjusting forest stand structure.Despite its promising results, this study is limited by the relatively small sample size and the specific forest types analyzed, which may constrain the generalizability of the findings.Future research should explore the integration of multi-temporal LiDAR datasets to assess dynamic changes in forest spatial structures and expand the methodology to diverse forest ecosystems.

Keywords: point cloud fusion; forestry resource information; point cloud segmentation; forest parameter extraction; spatial structure of stand

Address: R. Wang, K. Liu, Y. Li, T. T. Anni, X. Li, B. Bao, H. Hao, College of Forestry, Northwest A&F University, Yagling 712100, China, e-mail: hhk2018@126.com
* corresponding author

Introduction

The spatial structure of forests, defined as the spatial arrangement of trees and their attributes within a forest community, significantly influences the stability, development potential, and management scale of the forest (An, 2023). It plays a critical role in stand structure optimization (Dong & Liu, 2012; Zhang et al., 2014) and sustainable forest management and development (Hu, 2010). Furthermore, multivariate analysis of forest stand spatial structure can enhance the understanding of its distribution patterns, thereby providing a scientific basis for forest management and decision-making.Obtaining spatially explicit individual tree information is a prerequisite for assessing and evaluating forest spatial structure. Consequently, advancing smart forestry by rapidly and accurately acquiring individual tree data and achieving automated spatial structure parameter retrieval is essential (Chen, 2017; Fu, 2010; Liu et al., 2024). Previous studies have extensively explored quantitative indicators such as the Uniform Angle Index (W), which measures the spatial distribution pattern of trees (e.g., random, clustered, or evenly spaced), Mingling Degree (M), which assesses the degree of species mixing, Crowding Degree (C), which reflects the overlap of tree crowns and competition for space, and Neighborhood Comparison (U), which evaluates size differentiation among neighboring trees.For instance, Li et al. (2013) validated the independence of various structural parameters in characterizing tree attributes through an analysis of mixed broadleaf-Korean pine and natural pine-oak forests. Zhang et al. (2019) conducted an in-depth analysis of the multivariate distribution of spatial structure parameters in natural mixed forests of *Quercus aliena var. acuteserrata*, providing foundational data and reference for stand structure adjustment and optimization. Similarly, He et al. (2021) employed multivariate distribution methods to investigate the spatial structure characteristics of secondary *Betula platyphylla* forests.However, these studies predominantly rely on field-measured data, such as tree positions, diameter at breast height (DBH), and tree height, which involve substantial labor and high costs (Hui et al., 2016). Moreover, such measurements can cause disturbances to forest ecosystems, thereby limiting the applicability of these methods across broader regions.

Passive optical remote sensing enables the rapid acquisition of large-scale imagery, providing surface information of the target area through the optical properties of the images. This technology allows for the efficient retrieval of key forest attributes such as canopy closure (Hu et al., 2017; Li et al., 2016) and stand volume (Yang et al., 2016). Visible light remote sensing through unmanned aerial vehicles (UAVs) provides benefits such as cost-effectiveness, high-resolution imagery, and operational flexibility, making it highly suitable for precision forest monitoring(Bai et al., 2021). However, visible light data lacks penetration through the forest canopy, limiting its ability to capture information on vertical forest structure (Zeng, 2019). In comparison, LiDAR (Light Detection and Ranging) demonstrates greater potential for forest spatial structure analysis due to its canopy penetration capability (Xie et al., 2020) and high precision (Cao et al., 2019), making it a promising tool for acquiring stand spatial structure parameters (Chen, 2020). Despite its advantages, UAV-based LiDAR (UAV-LiDAR) operates with a top-down scanning approach, which limits its ability to accurately capture understory vegetation. Conversely, backpack-based LiDAR (BLS), which utilizes a bottom-up scanning method, faces challenges in dense and complex stands where canopy occlusion prevents the acquisition of upper-layer structure information.The integration of UAV-LiDAR and BLS data can mitigate these limitations, fully leveraging LiDAR's capability for high-precision forest parameter extraction. For instance, Zhang et al. (2020) improved tree height estimation by merging UAV-derived point clouds with terrestrial point clouds. Xu(2022) combined UAV and terrestrial laser scanning (TLS) data to estimate forest aboveground biomass, demonstrating the advantages of fused data in individual tree biomass estimation. Similarly, Shimizu et al. (2022) and Xu (2018) integrated airborne and terrestrial LiDAR point clouds, significantly enhancing parameter extraction accuracy. Yu et al. (2024)fused ALS (Airborne Laser Scanning) and TLS data, constructing 3D tree models that markedly improved the precision of branch attribute extraction and timber volume prediction.In summary, current LiDAR technologies for non-destructive acquisition of stand and individual tree parameters have matured significantly.By integrating multi-source LiDAR data, it becomes possible to leverage the complementary strengths of these systems: Airborne LiDAR excels in capturing large-scale canopy structures, while Backpack LiDAR provides detailed ground-level information. This fusion approach addresses key limitations of single-source data, enhancing the accuracy and comprehensiveness of spatial structure analysis. However, research on analyzing forest stand spatial structure characteristics based on the multivariate distribution of fused LiDAR data and spatial structure parameters remains limited.

Although advances have been made using remote sensing technologies such as LiDAR and UAVs to study forest structures, there is a lack of comprehensive studies focusing on the combination of UAV and Backpack LiDAR Scanning (BLS) for spatial structure analysis in coniferous forests, especially in the Qinling area. Current studies often fail to capture the fine-scale spatial patterns or consider multi-source data fusion for more accurate analysis. Forest ecosystems play a crucial role in global climate change, species conservation, and ecological restoration, with research on forest stand structure being key to understanding forest ecological processes. Particularly in the Qinling Mountains, this ecological corridor is vital for biodiversity conservation and climate regulation in central China.

Therefore, this study focuses on eight sample plots within the Huoditang Experimental Forest Farm in the Qinling Mountains, encompassing a total of 291 individual trees. UAV-LiDAR and backpack LiDAR point cloud data were collected and fused using multi-feature point matching and the Iterative Closest Point (ICP) algorithm. The fused point cloud was segmented using the relative shortest path algorithm, enabling the automated extraction of individual tree parameters.The purpose of this study is to develop and validate a multi-source LiDAR data fusion methodology for accurate and efficient extraction of forest spatial structure parameters. By applying this methodology to sample plots in the Huoditang Experimental Forest Farm, this research aims to: 1) highlight the potential of LiDAR data fusion in overcoming traditional survey limitations; 2) demonstrate its applicability in Coniferous forest ecosystems; and 3) provide insights into optimizing forest spatial structure for sustainable management and ecological stability.

Materials and methods

Study area

The study area is located within the Huoditang Experimental Forest Farm of Northwest A&F University (Fig. 1). The forest farm is located on the southern slope of the central Qinling Mountains in Ningshan County, Shaanxi Province, China, between 33°18'–33°28'N latitude and 108°21'–108°39'E longitude. The total area of the forest farm is approximately 22.25 km², with elevations ranging from 1,420 m to 2,474 m and slopes varying between 20° and 50°. This region experiences a subtropical humid monsoon climate, with an average annual temperature

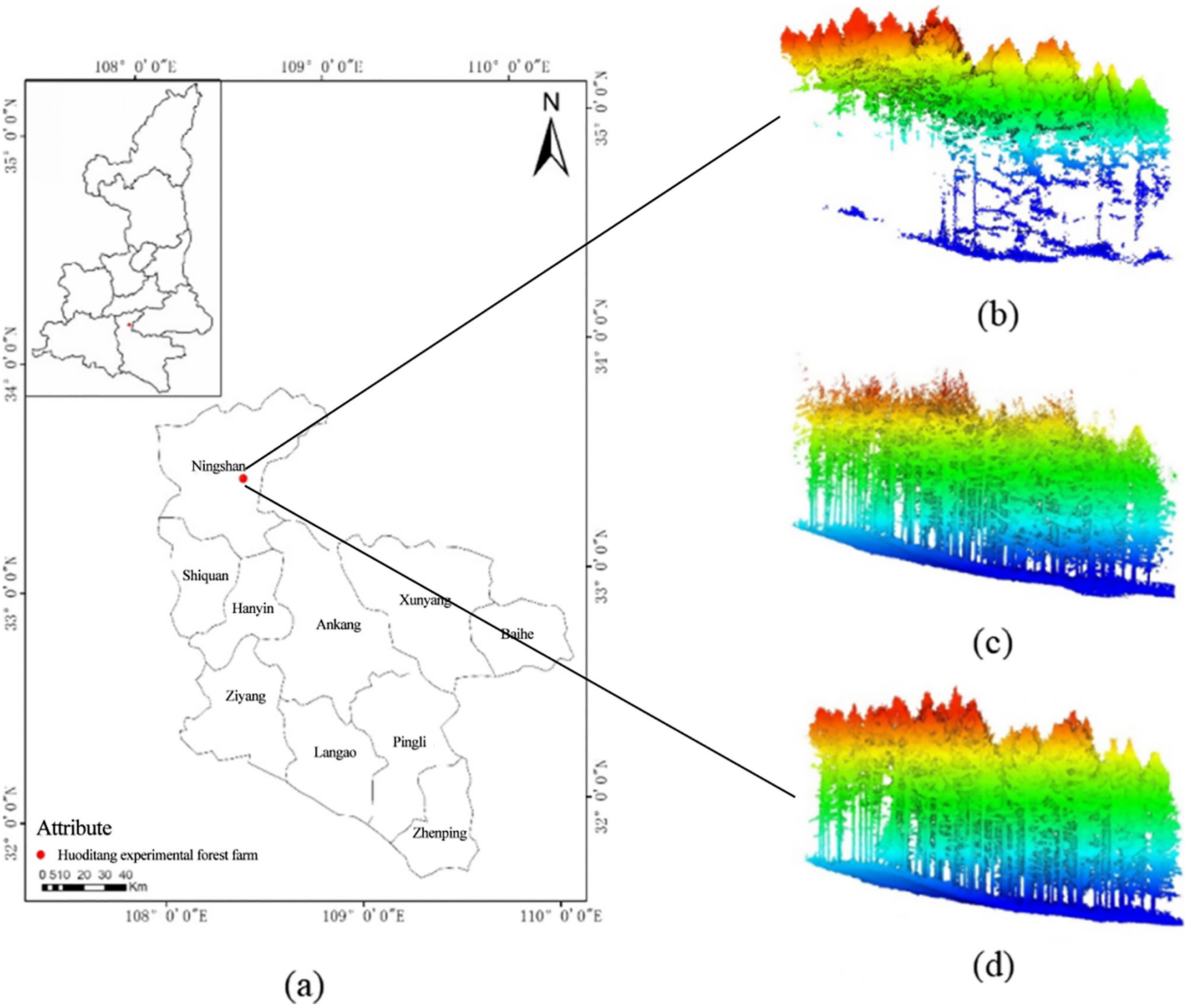

Fig. 1. Cloud data of the study area and sample sites (a) Geographical location of the study area; (b) Airborne LiDAR point cloud data; (c) Backage-LiDAR point cloud data; (d) Fusion point cloud data

of approximately 10.5 °C. The recorded extreme temperatures range from a minimum of −9.5 °C to a maximum of 35 °C, and the average frost-free period is around 199 days. The area receives an average annual precipitation of approximately 1,000 mm, primarily concentrated between July and September, and the average annual humidity is about 77%. The growing season for vegetation lasts approximately 177 days.

Data acquisition

UAV-LiDAR data

The data were collected in July 2023 using a DJI M300 RTK unmanned aerial vehicle (UAV) equipped with a high-precision LiDAR sensor (ZENMUSE L1). The L1 sensor operates at a laser wavelength of 905 nm, with a maximum of three echoes, a laser divergence angle of (0.03° × 0.28°) mrad, and a ranging accuracy of ± 3 cm. The UAV's flight path was designed using DJI Pilot software. Due to the significant topographic variation in the Qinling Mountains, a terrain-following flight mode was utilized to ensure consistent data acquisition over the complex terrain. The relative flight altitude was set to 100 meters, with a flight speed of 10 m/s, and both the forward and side overlap were set to 80%. These flight parameters ensured the collection of high-density and accurate LiDAR point clouds, which were crucial for the subsequent spatial structure analysis of the forest in the study area.

Backpack-LiDAR data

The BLS data and UAV-LiDAR data were collected simultaneously in July 2023 using the Feima Mobile LiDAR Scanning System SLAM100. This system is equipped with a 360° rotating gimbal, providing a 270° × 360° laser field of view, and features 16 laser channels with a point frequency of 320 kpts/s. The minimum measurement range of the system is from 0.5 to 120 meters, with a measurement error of ± 2 cm. Each sample plot was scanned along a closed-loop path to ensure the comprehensive capture of all tree information while minimizing data redundancy.

Field inventory data

The plot data were collected in July 2023 at the Huoditang Experimental Forest Farm of Northwest A&F University. The study plots were set at 20 × 30 m in size, and each tree within the plots was individually measured, with the minimum diameter at breast height (DBH) for measurement set at 5 cm. The positions of individual trees and the four boundary points of the plots were recorded using an RTK system (Zhonghaida - Haixingda vRTK2). The DBH was measured using a standard diameter tape, while the crown width (CW) was measured with a long tape to determine the east-west and north-south directions of the tree crown's vertical projection. Tree height was measured using a laser rangefinder.A total of 291 trees were surveyed across the eight plots. Based on visibility, understory vegetation, and canopy closure, the plots were classified into three simple plots (L3, L4, L5), two moderate plots (L1, L2), and three complex plots (Q1, Q2, Q3). Simple plots had lower canopy closure, with minimal tall shrubs in the understory and an open view. Complex plots had high canopy density, dense understory vegetation, and poor visibility. Moderate plots exhibited understory vegetation density and visibility conditions between the two extremes. Detailed information for the plots is provided in Table 1.

In the table, n refers to the number of trees measured in the plot. The data for tree height and diameter at breast height (DBH) in the table are presented as mean ± standard deviation.

Table 1. Detailed information of the plots

Plot number	Tree species	H (m)	DBH (cm)	Elevation (m)	Crown density	Understory environment	Complexity degree
L1 (n = 47)	*Larix principis-rupprechtii Mayr*	20.6±3.0	22.0±5.9	1999	0.75	simple	moderate
L2 (n = 37)	*Larix principis-rupprechtii Mayr*	21.5±1.6	22.6±4.5	1997	0.73	simple	moderate
L3 (n = 23)	*Larix principis-rupprechtii Mayr*	20.2±4.2	23.7±5.0	2013	0.55	simple	simple
L4 (n = 21)	*Larix principis-rupprechtii Mayr*	17.4±6.5	22.3±6.1	2013	0.43	simple	simple
L5 (n = 27)	*Larix principis-rupprechtii Mayr*	18.2±7.0	22.8±5.0	2013	0.53	simple	simple
Q1 (n = 58)	*Picea wilsonii*	23.5±2.5	25.6±5.2	2027	0.90	complex	complex
Q2 (n = 51)	*Picea wilsonii*	21.7±4.1	27.0±8.8	2025	0.86	complex	complex
Q3 (n = 27)	*Picea wilsonii*	17.6±4.3	28.5±7.6	2029	0.80	complex	complex

Research methodology

Species Composition and Spatial Structure Units

The main tree species in the study plots are *Picea wilsonii* and *Larix principis-rupprechtii Mayr* , with three plots dominated by *Picea wilsonii* and five plots dominated by *Larix principis-rupprechtii Mayr*. *Picea wilsonii* is a coniferous tree species in the spruce genus of the pine family, characterized by a conical crown, tall stature, and deep green foliage. It is an ideal species for establishing water conservation forests, and is primarily found in the mountainous and plateau areas of northwestern China, including provinces such as Gansu, Qinghai, Ningxia, and Shaanxi. *Larix principis-rupprechtii Mayr*, also known as Siberian larch, is an important ornamental tree species. Additionally, *Larix principis-rupprechtii Mayr* absorbs a significant amount of carbon dioxide during its growth, which contributes to mitigating global warming and plays a crucial ecological role. The *Larix principis-rupprechtii Mayr* plantation in the Huoditang Experimental Forest Farm was established in the mid-1970s, and no harvesting or replanting has been conducted since its establishment.The size of the spatial structure unit is determined by the reference tree and its neighboring trees. According to Hui et al., the spatial structure unit consisting of the reference tree and its four closest neighboring trees (n = 4) is most suitable for describing the structural characteristics of a forest stand [1]. Therefore, in this study, a spatial structure unit is defined by one reference tree and four neighboring trees, with the standard angle α_0 set to 72°. To eliminate the edge effect, a 2-meter buffer zone was set around the perimeter of the plots. Trees within the buffer zone can only participate as neighboring trees in the analysis, while trees within the central area can serve as either reference trees or neighboring trees for the analysis.

UAV-LiDAR and backpack-LiDAR matching

After preprocessing the UAV-LiDAR and BLS point cloud data, the UAV-LiDAR data is used as a reference to perform rough registration of the BLS point cloud. Initially, the two point clouds from the same scene are roughly aligned through rotation or translation of the initial matrix values. Then, a multi-feature point matching method is applied to find corresponding feature points between the two point cloud datasets, achieving preliminary alignment. The multi-feature point matching method is based on feature points in the point cloud that exhibit significant differences in shape, curvature, or other attributes, which can be used to uniquely identify the local structure of the point cloud.Subsequently, the Iterative Closest Point (ICP) algorithm is employed for fine registration of the point clouds. The core idea of the ICP algorithm is to iteratively minimize the difference between the point clouds in order to achieve precise alignment. The main steps include: initialization, matching corresponding points, calculating the optimal transformation, performing rigid body transformation, and checking for convergence.

Single tree segmentation, parameter extraction, and accuracy verification

The study used the density-based spatial clustering algorithm with noise (DBSCAN) for tree trunk segmentation (robustness to noise points and high efficiency. The comparative shortest-path (CSP) algorithm was applied for point cloud normalization (Sun et al., 2013), DBH estimation, and crown segmentation.

For the comparison between detected trees and field-measured trees, a 1:1 matching approach was adopted. The accuracy of the segmentation was verified using metrics such as correct segmentation count Nt, missed segmentation count N*o*, over-segmentation count Nc, detection rate r,precision p,and F1 score. In the buffer zone, if there is only one extracted tree crown apex, this extracted value is considered a true positive (TP). If there are multiple extracted vertices, the one closest to the field-measured location is selected as the true positive (TP), and the others are regarded as false positives (FP). If no extracted vertex is present within the buffer zone, the tree is considered a false negative (FN).The accuracy of tree diameter at breast height (DBH), tree height, and crown width extraction was evaluated using the coefficient of determination , root mean square error (RMSE), and mean absolute error (MAE) methods. The corresponding formula is:

$$r = \frac{N_t}{N_t + N_o} \tag{1}$$

$$p = \frac{N_t}{N_t + N_c} \tag{2}$$

$$\text{F1 score} = \frac{2{*}TP}{2{*}TP + FP + FN} \tag{3}$$

$$R^2 = 1 - \frac{\sum_{i=1}^{n}(\hat{x}_l - \bar{x})^2}{\sum_{j=1}^{n}(x_i - \hat{x})^2} \tag{4}$$

$$RMSE = \sqrt{\frac{1}{n}\sum_{i=1}^{n}(x_i - \hat{x}_i)^2} \tag{5}$$

$$MAE = \sum_{i=1}^{n}\left|\frac{x_i - \hat{x}_i}{n}\right| \tag{6}$$

where Nt refers to the number of trees detected within the sample plot, No represents the number of trees missed by the algorithm, and Nc denotes the number of trees detected in the plot that do not actually exist, x_i represents the ground truth value, $\hat{x}_i$ denotes the predicted value, and $\bar{x}$ is the mean of the measured values.

Indicators for evaluating the spatial structure of forest stands

The spatial structure of forest stands was analyzed by calculating the Zero-element, univariate, bivariate, and trivariate distributions of parameters such as W, U, and C extracted from the fused point cloud data. A comparative analysis was conducted between the N-order distribution of structural parameters derived from the original data and those extracted from the fused data, followed by validation of the structural parameters using field-measured data.

The zero-element distribution mainly describes the mean value characteristics of the spatial structure parameters of the stand. According to this distribution, the overall average status of forest spatial structure can be observed. The average W ($\overline{W}$) in the range of [0.475,0.517] belongs to random distribution, < 0.475 is uniform distribution, > 0.517 belongs to cluster-like distribution. The average U ($\overline{U}$) reflects the dominant degree of tree species in the stand, with the medium grade as the watershed, the smaller the value, the more disadvantaged the tree, and the vice versa. The average C ($\overline{C}$) is the medium level as the watershed. The higher $\overline{C}$, the denser and more continuous the forest canopy, and the greater the competitive pressure among trees.

The univariate distribution of forest stand spatial structure parameters is represented by the frequency distribution corresponding to five levels (0, 0.25, 0.50, 0.75, and 1), The corresponding formula is

$$p_i = P(X = x_i) \tag{7}$$

In the formula, ≥0 and the sum of all frequencies equals 1.

The bivariate distribution pairs spatial structure parameters based on different frequency levels (Wan et al., 2019), resulting in 25 combinations, each representing distinct structural characteristics. The distribution of their occurrence frequencies is then analyzed.

The trivariate distribution refers to combining the five levels of any two structural features with the five levels of another structural feature, and performing a cross-analysis to obtain the frequency distribution of 125 unique structural combinations (Wu et al., 2019).

The spatial structure parameters involved in this study (Table 2) were calculated using ArcGIS 10.2 software, plotted with Origin 2018 , and the frequency distribution was statistically analyzed using Office Excel 2018.

Results and analysis

Point cloud fusion results

After the coarse registration, the BLS point cloud and the UAV LiDAR point cloud are generally aligned, bridging the gap in the canopy structure missing in the reference point cloud. However, there are misalignments on the ground, which affect

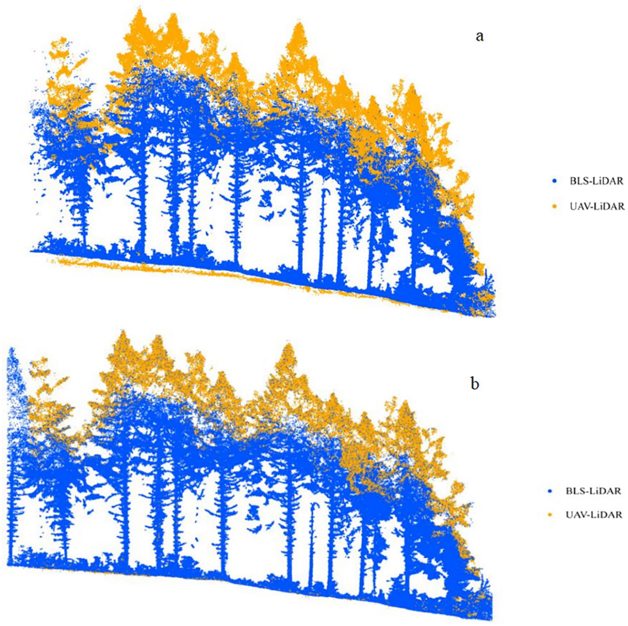

Fig. 2. Registration result of BLS point cloud and UAV point cloud. The yellow point cloud represents the BLS-LiDAR and the blue point cloud represents the UAV-LiDAR

Table 2. Calculation formula of spatial structure parameters.

Spatial structure parameters	Formula	Explaination
Uniform angle index	$W_i = \frac{1}{n}\sum_{j=1}^{n} Z_{ij}$	When the j-th angle α is less than 72°, Z_{ij} = 1; otherwise Zij = 0
Neighborhood comparison	$U_i = \frac{1}{n}\sum_{j=1}^{n} K_{ij}, k_{ij}$	If the j-th attribute of the neighboring tree is smaller than that of the reference tree i, then K_{ij} = 1; otherwise K_{ij} = 0
Crowding degree	$C_i = \frac{1}{n}\sum_{j=1}^{n} y_{ij}$	When the crown projection of the reference tree i overlaps with that of the neighboring tree j, y_{ij}=1; otherwise y_{ij} = 0.

subsequent tree height and diameter at breast height (DBH) measurements (Fig. 2a). The point cloud is then fine-tuned using the Iterative Closest Point (ICP) algorithm, resulting in the accurately registered point cloud (Fig. 2b). Compared to the coarse registration in Figure 2a, the ground point cloud's stratification phenomenon within the same plot has been eliminated, and the fusion of the canopy point cloud has improved. The Digital Elevation Model (DEM) of the fused point cloud was obtained using the Inverse Distance Weighted (IDW) interpolation method [28]. The UAV LiDAR point cloud (DEM_{UAV}) and the fused point cloud (DEM_Z) were compared by calculating the difference (DEM_c). The minimum value of DEM_c is 0.007 m, and the maximum value is 0.053 m, indicating that the vertical precision is at the centimeter level and the vertical alignment of the point clouds is highly accurate.

Single tree detection and parameter extraction results

A total of 291 individual trees were measured across eight sample plots, with 289 trees successfully detected and matched on a one-to-one basis. The accuracy of individual tree position recognition reached 92.9%, and the overall F-measure was 96.0%. Two trees were missed (0.69% of the total trees), and 22 trees were over-detected, with only one being a *Larix principis-rupprechtii Mayr*, while most over-detected trees were found in the *Picea wilsonii* plots with higher density and more understory shrubbery. This led to the misdetection of shrubs taller than 1.3 meters as trees. The segmentation accuracy of the fused point cloud decreased as the number of trees, understory canopy, and plot complexity increased. The main reason for this was that in the complex plots (Q1, Q2, Q3), the understory environment was complicated with taller shrubs that intertwined with tree trunks, resulting in missegmentation. In contrast, simpler and moderate plots had fewer shrubs, leading to better ground segmentation. The detailed results for individual tree detection in each plot are shown in Table 3.

Based on the fused point cloud data, the R^2 for diameter at breast height (DBH) extraction in the simple plot (Fig. 3a) was 0.98, with RMSE of 0.81 cm and MAE of 0.62 cm. In the moderate plot (Fig. 3b), the R^2 was 0.95, with an RMSE of 1.22 cm and an MAE of 0.70 cm. In the complex plot (Fig. 3c), the R^2 was 0.92, with an RMSE of 2.01 cm and an MAE of 1.22 cm.

Based on the fused point cloud data, the tree height extraction results in the simple plot (Fig. 4a) showed an R^2 of 0.99, RMSE of 0.55 m, and MAE of

Table 3. Single tree extraction accuracy results of fusion point cloud

Plot number	Tree species	Number of measured individual trees	Number of extracted individual trees	FP	FN	TP	r(%)	p(%)	F(%)
L1	*Larix principis-rupprechtii Mayr*	47	42	0	0	47	100.0	100.0	100.0
L2	*Larix principis-rupprechtii Mayr*	37	37	0	0	37	100.0	100.0	100.0
L3	*Larix principis-rupprechtii Mayr*	23	23	0	0	23	100.0	100.0	100.0
L4	*Larix principis-rupprechtii Mayr*	21	22	1	0	21	100.0	95.5	97.7
L5	*Larix principis-rupprechtii Mayr*	27	27	0	0	27	100.0	100.0	100.0
Q1	*Picea wilsonii*	58	66	9	1	57	98.3	86.4	91.9
Q2	*Picea wilsonii*	51	62	11	0	51	100.0	82.3	90.3
Q3	*Picea wilsonii*	27	27	1	1	26	96.3	96.3	96.3
Sum		291	311	22	2	289	99.3	92.9	96.0

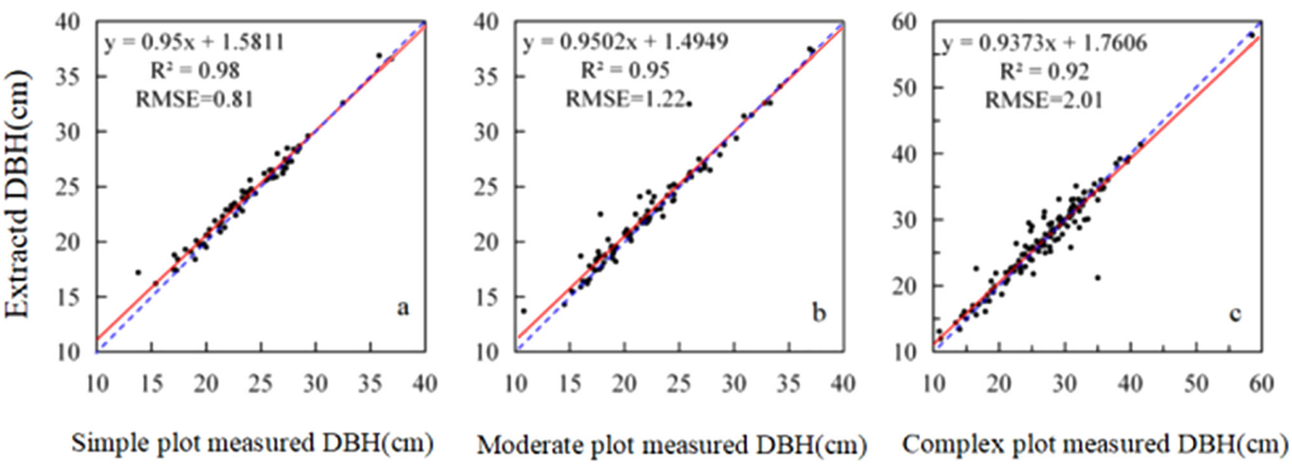

Fig. 3. Extraction accuracy results of DBH

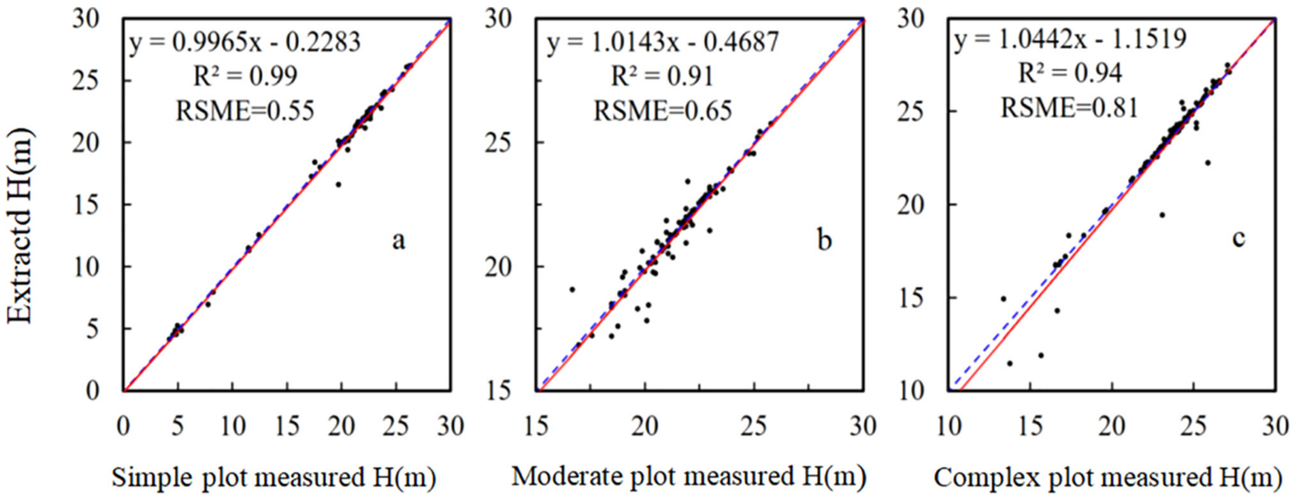

Fig. 4. Extraction accuracy results of heigh

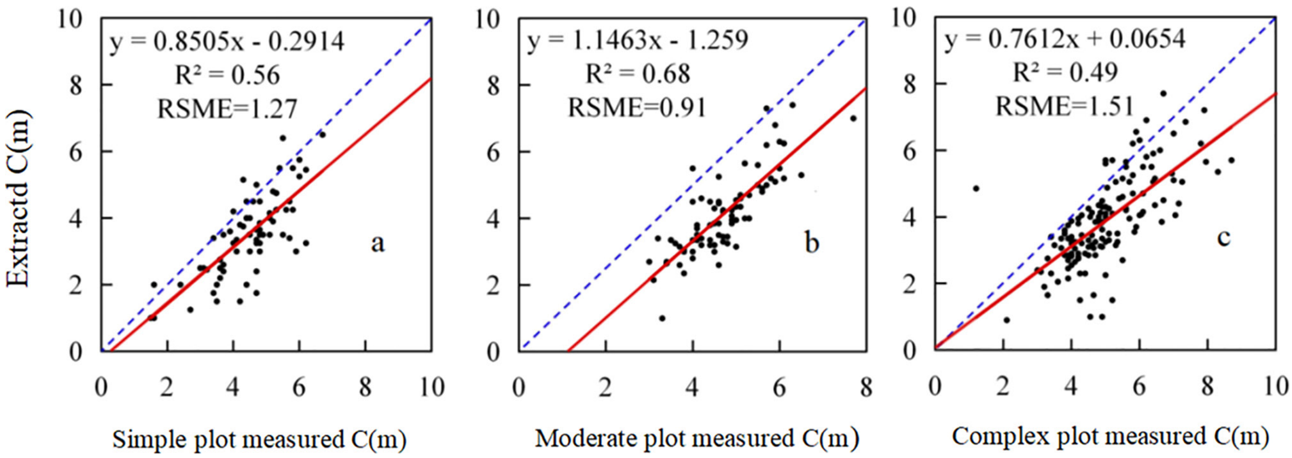

Fig. 5. Accuracy results of crown width

0.34 m; in the moderate plot (Fig. 4b), the R^2 for tree height extraction was 0.91, with RMSE of 0.65 m and MAE of 0.38m; and in the complex plot (Fig. 4c), the R^2 was 0.94, RMSE was 0.81 m, and MAE was 0.85 m.

Based on the fused point cloud data, in the simple plot (Fig. 5a), the crown width extraction resulted in an R^2 of 0.56, RMSE of 1.27m, and MAE of 1.03m. In the moderate plot (Fig. 5b), the crown width extraction showed an R^2 of 0.68, RMSE of 0.91m, and MAE of 0.78m. In the complex plot (Fig. 5c), the R^2 was 0.49, RMSE was 1.51 m, and MAE was 1.24 m.

Zero-element distributions

The average values of three structural parameters – W, U, and C – are presented in Table 4. In terms of stand-level distribution, the L1 and L3 plots in the *Larix principis-rupprechtii Mayr* forest show a random distribution ($\overline{W} \in [0.475, 0.517]$). The L2 and L5 plots have an average $\overline{W} \in [0, 0.475]$, indicating an even distribution, while plot L4 exhibits a clumped distribution ($\overline{W} > 0.517$). In the spruce forest, two plots (Q2, Q3) display a random distribution, while plot Q1 shows an even distribution. Overall, both larch and spruce forests have an average $\overline{W}$ value of 0.48, indicating a random distribution ($\overline{W} \in [0.475, 0.517]$). Regarding size differentiation, the *Larix principis-rupprechtii Mayr* forest has an of 0.50, and *Picea wilsonii* forest has an $\overline{U}$ of 0.47. Both forests are in a moderate state ($\overline{W} \in (0.25, 0.5]$), suggesting a general level of competition and that the size differentiation is not pronounced. In terms of density, the average C of the *Larix principis-rupprechtii Mayr* forest is 0.75, while

Table 4. Zero-element distribution of stand spatial structure in sample plots

Plot number	L1	L2	L3	L4	L5	Sum	Q1	Q2	Q3	Sum
W	0.51	0.43	0.50	0.61	0.39	0.48	0.45	0.49	0.51	0.48
U	0.51	0.46	0.40	0.47	0.50	0.48	0.46	0.48	0.48	0.47
C	0.93	0.88	0.54	0.64	0.32	0.75	0.96	0.91	0.93	0.94

that of the *Picea wilsonii* forest is 0.94. This indicates that both forests are relatively dense, with the *Picea wilsonii* forest being denser than the *Larix principis-rupprechtii Mayr* forest.

Univariate distribution

The univariate distribution is obtained by using a single spatial structure parameter (W, U, C) and its relative frequency distribution across different classes. From the univariate distribution charts (Fig. 6), it can be observed that in the *Larix principis-rupprechtii Mayr* sample plots (Fig. 6a) and *Picea wilsonii* sample plots (Fig. 6b), the majority of the trees are randomly distributed, accounting for about 50% in both cases. The next largest proportion of trees are in a uniform state, with a percentage ranging from 25% to 30%. The third largest group consists of trees in a very uneven state, accounting for 17.89%. Trees in very uneven or very uniform states are fewer, each accounting for less than 4%, indicating that the overall tree distribution is random. The Neighborhood Comparison (U) is relatively evenly distributed across the classes, with no extreme values in terms of frequency, indicating a uniform size differentiation of the trees, with no significant dominance or subordination of individual trees. The Crowding Degree (C) shows a gradually increasing trend in the distribution at values of 0, 0.25, 0.5, 0.75, and 1 (representing very

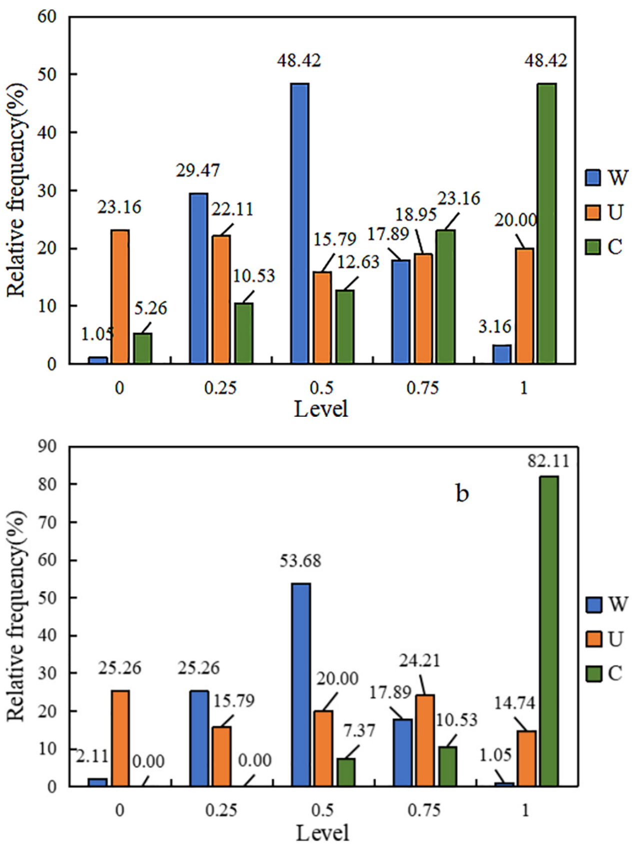

Fig. 6. Unitary distribution

sparse, sparse, moderately dense, quite dense, and very dense, respectively). This suggests that the tree crowns in the reference trees' microenvironment are tightly spaced, and there are many instances of continuous tree crowns between the reference tree and the nearest neighboring tree, indicating intense competition among the trees in the sample plot.

Binary distribution

Binary distribution utilizes two structural parameters (W, U, C) in combinations to describe, forming three combinations: W-U, W-C, and U-C (Fig. 7). As shown in Figure 6, most of the trees in *Larix principis-rupprechtii Mayr* forests (Fig. 7a, 7c) and *Picea wilsonii* forests (Fig. 7b, 7d) are randomly distributed (W = 0.5), with the relative frequency gradually decreasing towards the two extreme states of very uniform (W = 0) and very uneven (W = 1), which roughly follows a normal distribution. The relative frequency value is highest when W = 0.5, indicating that the majority of trees in the stand are randomly distributed. In the W-C chart, it can be seen that when *Larix principis-rupprechtii Mayr* (Fig. 7c) and *Picea wilsonii* (Fig. 7d) are at the same level of W, the frequency of C is highest at the "fairly dense" (C = 0.75) and "very dense" (C = 1) levels. The cumulative relative frequencies of the light blue and yellow bars in the figure are 48% and 23% for *Larix principis-rupprechtii Mayr* and 82% and 11% for *Picea wilsonii*, respectively, indicating that both *Larix principis-rupprechtii Mayr* and *Picea wilsonii* Mast. stands are highly dense. From the U-C chart, the combination of U and C is mostly located on the upper ridge (C = 0.5), suggesting that both *Larix principis-rupprechtii Mayr* and *Picea wilsonii* face intense competition.

Ternary distribution

The ternary distribution analysis using common spatial structure parameters, including U, W, and C, reveals similar distribution patterns for *Larix principis-rupprechtii Mayr* (Fig. 8) and *Picea wilsonii* (Fig. 9). Figure 8a, 8b, 8c, 8d, and 8e represent the five distribution states of *Larix principis-rupprechtii Mayr* trees under the W-U bivariate distribution with varying levels of C: 0 (very sparse), 0.25 (sparse), 0.5 (moderately dense), 0.75 (fairly dense), and 1 (highly dense). Similarly, Figure 9a, 9b, 9c, 9d, and 9e show the corresponding distribution states for *Picea wilsonii* under the same W-U bivariate distribution.For *Larix principis-rupprechtii Mayr*, the trees predominantly exhibit a random distribution to highly dense growth with a dominance of absolute disadvantage, with the highest frequency of distribution observed at C = 0.75 and C = 1, indicating that the forest stands are relatively dense to highly dense. As observed in Figure 7, at the same U-C level, the frequency of random distribution (W = 0.5) is the highest for *Larix principis-rupprechtii Mayr*, suggesting that most trees follow a random distribution. In contrast, *Picea wilsonii* stands are mostly characterized by random distribution transitioning to high density, with the highest frequency observed at C = 1 (Fig. 8e), signifying highly dense tree stands. Notably, there

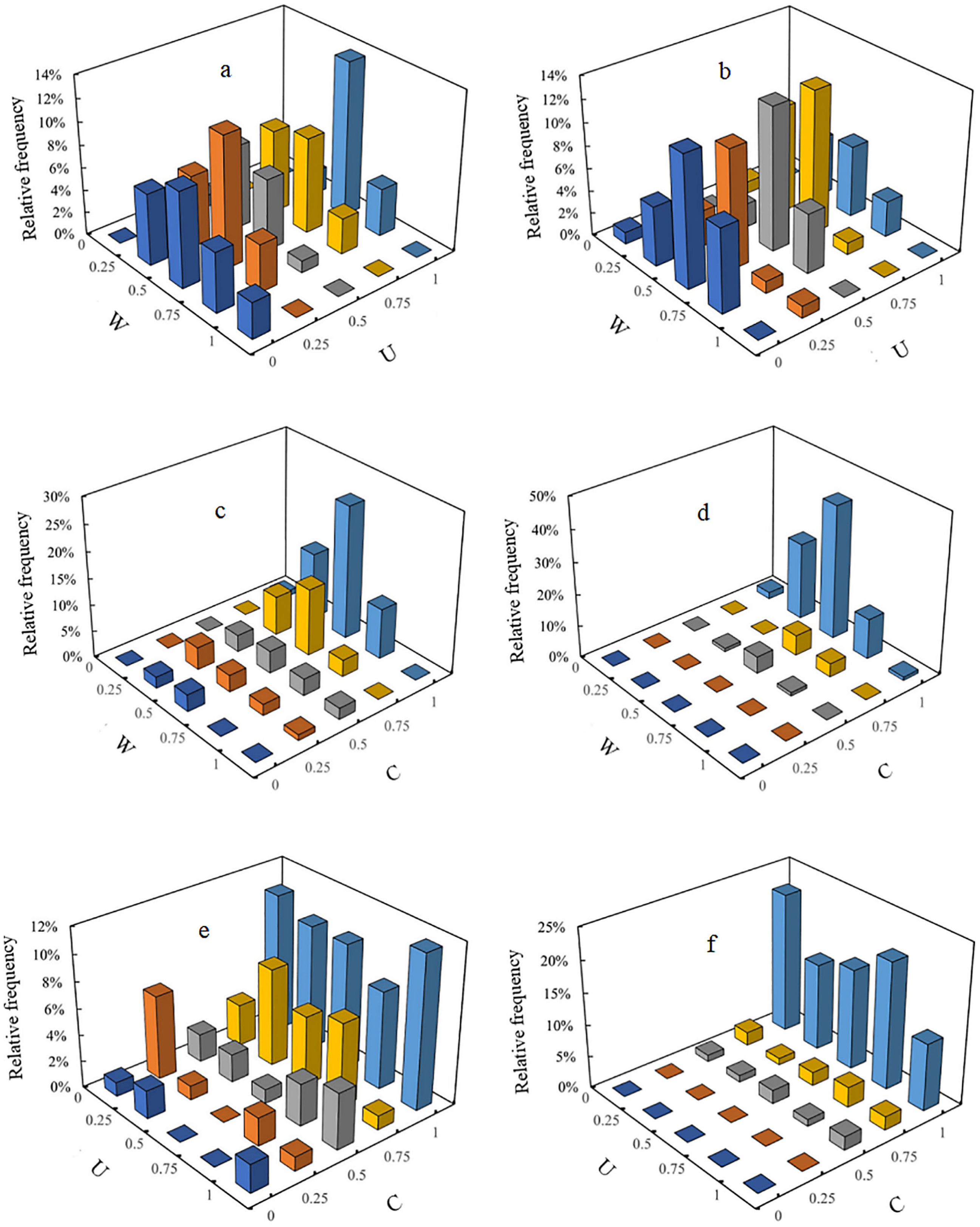

Fig. 7. Binary distribution

is no distribution observed at C = 0 (Fig. 9a) and C = 0.25 (Fig. 9b) for Picea wilsonii, indicating the absence of sparse trees in these plots, with the majority of trees distributed in a dense pattern.

Considering that the W serves as a key indicator for determining tree distribution patterns, when W = 1, the trees are very densely clustered, with intense competition among individual trees, resulting

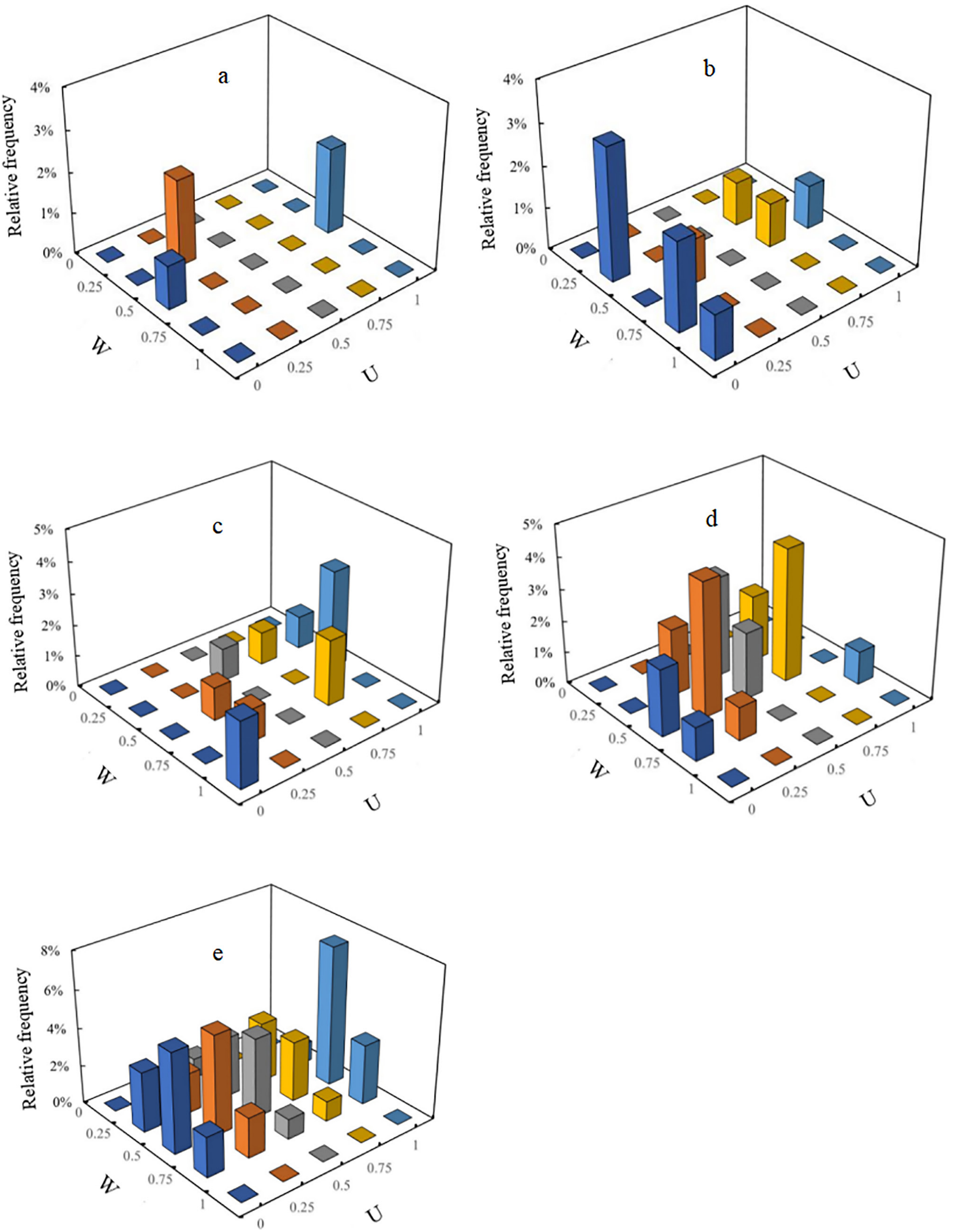

Fig. 8. Ternary distribution of stand spatial structure of *Larix principis-rupprechtii Mayr*

in poor stand stability. The U reflects the dominance status of trees within a stand, where U = 0 indicates that the trees are in a dominant class, with strong competitive ability, occupying a large share of the available resources and suppressing the growth of neighboring trees. The Crowding Degree (C) indicates the degree of crowding between trees; a higher value represents higher spatial utilization. A

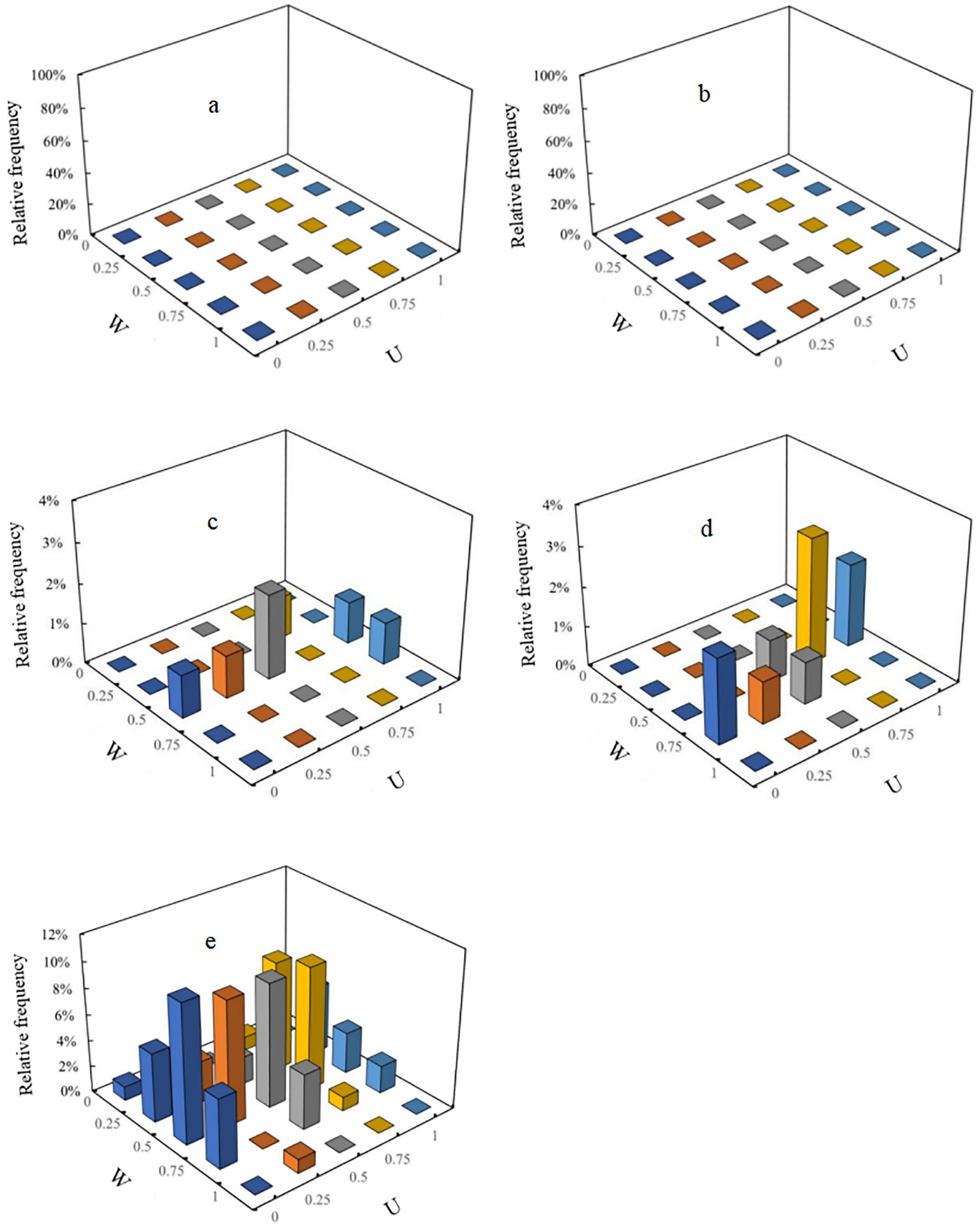

Fig. 9. Ternary distribution of stand spatial structure of *Picea wilsonii*

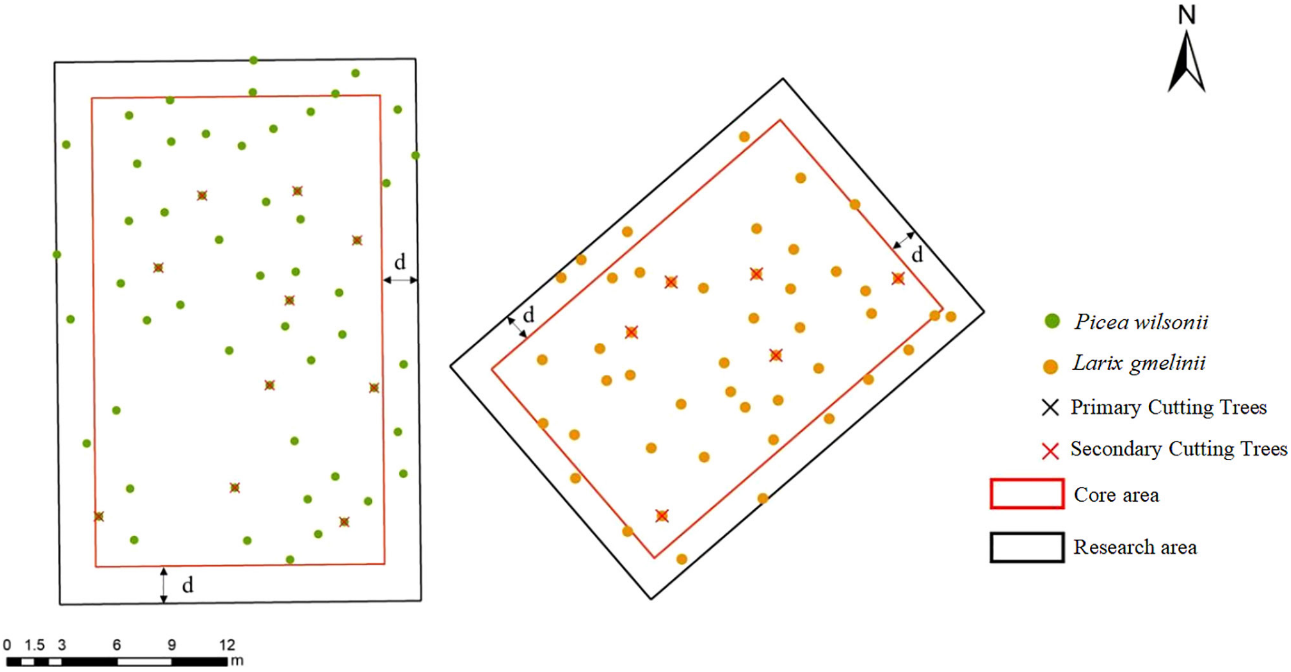

Fig. 10. Schematic diagram of thinning forest. d is the buffer width, d = 2 m

Table 5. Statistics of potential harvested trees

Plot number	L1	L2	L3	L4	L5	Q1	Q2	Q3	Sum
Primary Cutting Trees	0	0	0	0	0	0	0	0	0
Secondary Cutting Trees	6	5	1	1	0	10	8	4	35

reasonable crowding degree ensures that the stand's space is effectively utilized while maintaining a balance where trees can grow without negatively affecting each other. When C = 1, the stand is overly dense, with high crown overlap, which negatively impacts the potential growth of trees.Based on these criteria, the harvesting decision-making process is formulated as follows: trees that meet all three conditions (W = 1, U = 0, C = 1) are defined as primary cutting trees, while those that meet any two of the three conditions are categorized as secondary cutting trees. This approach results in the potential logging tree statistics (Table 5) and a schematic diagram of thinning harvesting in *Larix principis-rupprechtii Mayr* and *Picea wilsonii* sample plots (Fig. 10).

Discussion

Multivariate distribution of stand spatial structure parameters based on fused point cloud

Traditional methods for obtaining forest parameters and stand spatial structure data often rely on field surveys, which require extensive manual measurements of tree height, diameter at breast height (DBH), crown width, and other information. These methods are labor-intensive, costly, time-consuming, and not conducive to the further application of stand spatial structure research. This study uses fused point cloud data as the source, offering high precision in identifying and labeling individual tree positions, thus providing a convenient means for studying stand spatial structure and the precise localization of harvested trees.The study employs multi-source LiDAR data and applies point cloud segmentation methods to extract tree parameters. The RMSE for the extraction of DBH is 1.58 m, crown width is 1.3 m, and tree height is 1.21m. Additionally, single-source BLS point cloud data were used for individual tree segmentation, with RMSE values for DBH extraction at 1.63 cm, crown width at 1.62 m, and tree height at 1.21 m. The fused point cloud extraction of crown width and tree height shows substantial improvements in accuracy over the BLS point cloud, with notable increases in R^2 and reductions in RMSE. UAV-LiDAR compensates for gaps in canopy data from BLS point cloud scanning.To verify whether the accuracy of single-tree point cloud information obtained from the fused data affects the stand spatial structure parameters, the Kolmogorov-Smirnov (K-S) test was used to compare the stand spatial structure parameters calculated from the extracted point cloud data with those derived from actual measurements. The null hypothesis for this test is that both sample sets originate from the same population. Validation or rejection of this hypothesis helps identify any influencing factors.As shown in Table 6, the K-S test for the and parameters yields P-values of 1.00 (P > 0.05), indicating no significant differences. However, the K-S test for the parameter yields a P-value of 0.00 (P < 0.05), primarily due to the lower accuracy of crown extraction during individual tree segmentation. Aside from density, no significant differences were observed for the other parameters.Subsequently, multivariate distribution calculations for stand spatial structure parameters were performed using both detection data and actual measurement data. A paired t-test was applied to assess whether there were significant differences between the multivariate distributions obtained from the single-tree point cloud data and those derived from actual measurements. According to Table 7, the t-test results for *Larix principis-rupprechtii Mayr* stand structure extraction and actual values show P-values greater than 0.05, indicating no significant differences. Similarly, Table 8 shows that for Picea wilsonii stands, the multivariate distribution t-test results also indicate no significant differences (P > 0.05). This demonstrates that single-tree point cloud information extracted from fused point cloud data can be effectively used for multivariate distribution analysis of stand spatial structure. Other scholars have conducted studies on forest stand spatial structure using field-measured data from the Huoditang Experimental Forest Farm. Their research indicates that the horizontal spatial distribution pattern of coniferous forests in the Huoditang region is predominantly random or clumped, with random distribution accounting for more than 50%. The diameter at breast height (DBH) is uniformly distributed, and U is dominated by dominant and subdominant trees. The mingling degree shows that the spatial isolation of tree species is primarily concentrated at moderate mingling levels or higher, with high crowding levels, which is consistent with the results of this study (Zhang et al., 2014; Shi et al., 2008). Therefore, utilizing fused point cloud data (U-T LiDAR) to analyze the spatial structure of artificial coniferous forests yields results that differ minimally from field survey data, suggesting that it can further replace field measurement methods.

The use of LiDAR point cloud data fusion technology for multi-variable distribution analysis of forest spatial structure parameters offers significant advantages. This method can construct a three-dimensional network of trees within a forest through a systematic process of measurement → extraction → calculation → screening → decision-making, integrating various parameters of forest structure, including detailed information such as precise tree locations. Additionally, it can quickly identify potential harvesting trees (Fig. 9), efficiently evaluating the spatial structure of the forest without the need for traditional field measurements such as inter-tree distances and angles. This method is more efficient than traditional approaches in determining the location of potential harvest trees, enhancing the feasibility of forest operations, significantly reducing survey costs, and enabling the collection of forest information over a larger area.

The limitation of this study is that the specific optimization degree of the stand spatial structure adjusted according to this suggestion is not clear. Only the tall trees in the stand are considered, and

Table 6. K-S test of the average value of spatial structure parameters

Parameters	*Larix principis-rupprechtii Mayr*		*Picea wilsonii*	
	Maximum Absolute Difference	P	Maximum Absolute Difference	P
W	0.044	1.000	0.011	1.000
U	0.033	1.000	0.054	1.000
C	0.300	0.000	0.516	0.000

Table 7. T-test of *Larix principis-rupprechtii Mayr* stand spatial structure

Type	Paired data	95% Confidence Interval		t	df	P value
		Lower Limit	Upper Limit			
Zero-element distributions	Extraction – Measured	−21.99%	32.71%	0.84	2	0.49
Univariate distribution	Extraction – Measured	−5.88%	5.88%	0.00	14	1.00
Binary distribution	Extraction – Measured	−0.86%	0.86%	0.00	74	1.00
Ternary distribution	Extraction – Measured	−0.23%	0.23%	0.00	123	1.00

Table 8. T-test of *Picea wilsonii* stand spatial structure

Type	Paired data	95% confidence interval		t	df	P value
		Lower limit	Upper limit			
Zero-element distributions	Extraction – Measured	−40.56%	26.41%	−0.91	2	0.46
Univariate distribution	Extraction – Measured	−9.12%	9.12%	0.00	14	1.00
Binary distribution	Extraction – Measured	−1.29%	1.29%	0.00	74	1.00
Ternary distribution	Extraction – Measured	−0.33%	0.33%	0.00	124	1.00

the effects of shrubs, herbs and ground cover on the stand spatial structure are not considered.Secondly, this study include the use of single temporal and spatial data, with a lack of data collection for multi-temporal and multi-spatial complexity datasets. The LiDAR point cloud data collected for this study lacks comprehensive seasonal and geographical coverage, as sampling and research were not conducted across different temporal and spatial sites. Future work could involve data collection for different forest types and seasons, dynamically monitoring key factors of forest spatial structure. On the other hand, this study did not perform single-tree classification and recognition on the fused data, lacking the extraction of mixed forest density and the identification of diseased and dead trees. Moreover, the spatial structure of the forest in this study mainly focuses on the horizontal distribution pattern of trees, lacking analysis of vertical structure; also, information such as the age of individual trees, diameter class and forest age were not added into the forest spatial parameter analysis, so as to obtain multivariate distribution characteristics of stand spatial structure at more levels. The spatial structure characteristics of horizontal direction and vertical direction were combined, which provided directions for future research.

Forest stand spatial structure parameter multivariate distribution analysisultivariate distribution of stand spatial structure parameters based on fused point cloud

The multi-dimensional distribution of spatial structure parameters provides important criteria for the precise selection of trees for forest management and harvesting. It not only reflects the degree of isolation between tree species, distribution patterns, and their crowding conditions, but also serves as a crucial basis for deciding which trees to retain or cut. This information allows for the optimization of the stand's spatial structure. From the results of the zero-element analysis, it can be observed that the majority of trees in coniferous forests are distributed randomly, in a moderate state, and tend to be relatively dense. The univariate distribution graph (Fig. 6) shows that the distribution of W at levels 0 and 1 is minimal, while the most frequent distribution occurs at 0.5. This suggests that absolute distribution structural units are rarely seen in coniferous forests, which is due to the fact that these stands are primarily secondary forests formed after disturbance on the basis of the original coniferous forests.From the univariate distribution of C, coniferous forest stands are generally in a highly dense state, with good growth conditions, but the trees are very close to each other, leading to significant canopy overlap. This results in poor light conditions for the trees in the lower canopy. Such a situation could slow down the natural regeneration speed under the canopy, which may be detrimental to the forest's sustainable development and management.From the analysis of the binary and ternary distributions, the multi-dimensional distribution refines the zero-element and univariate distributions. In these distributions, there are no trees with unreasonable values in all three structural parameters ($W = 1$, $U = 0$, $C = 1$), and 35 trees (about 12%) show two unreasonable parameters.When selecting trees for potential harvesting, the structural parameters should be taken into account, adjusting competition within the stand, spatial distribution patterns, and the degree of isolation between tree species. Regarding W, when the stand is generally randomly distributed, trees with a W greater than or equal to 0.75 should be selected as adjustment targets. Additionally, to reduce competition pressure on dominant trees and create more living space, trees with a Crowding Degree greater than 0.75 and a Neighborhood Comparison smaller than 0.25 should be selected as adjustment targets. By using this approach and integrating the multi-dimensional distribution results, the spatial structure of the stand can be adjusted to bring it closer to a natural state.

In conclusion, the following harvesting suggestions are proposed: The first round of harvesting should target dead standing trees and trees affected by pests and diseases. In the second, third, and fourth rounds, select trees that have unreasonable values in all three parameters, two parameters, and one parameter, respectively, as the harvesting targets. Simultaneously, conduct light thinning to open up growth space for the upper canopy trees, reduce canopy closure, and stand density, allowing the lower canopy trees to better utilize light, promoting growth and development, and enhancing stand regeneration.

Conclusions

The study uses eight 20 m×30 m coniferous forest plots at the Huoditang Experimental Forest Farm of Northwest A&F University as the research area to explore the multi-dimensional distribution analysis of spatial structure parameters based on fused point cloud data, and the following conclusions are drawn: 1) The point cloud fusion performs well, compensating for the point cloud gaps inherent in single-platform LiDAR data sources. The average DEM difference of each plot before and after the multi-platform point cloud fusion is less than 6 cm, with a standard deviation of less than 7 cm, achieving centimeter-level vertical accuracy. After registration, the positions of individual trees align closely with the field-measured locations, with coordinate differences all being less than 0.5 m, indicating good horizontal alignment of the fused point clouds. 2) The fusion of point clouds overcomes the shortcomings of a single data source, providing a more reliable guarantee for accurately extracting forest parameters. The overall detection rate of tree counts obtained from the fused point cloud is 99.3%, which is a 13% improvement compared to a single data source, and the F-measure is 96%, an improvement of 7.2%. The total accuracy for diameter at breast height (RMSE = 1.58 cm), tree height (RMSE = 1.21 m), and crown width (RMSE = 1.30 m) is the highest. Among the three sample plots, the individual tree detection rate is above 98%, the precision is greater than 82%, and the F-measure is above 90%. The correlation coefficient (R^2) for diameter at breast height extraction is greater than 0.92, the RMSE is less than 2.01 cm, and the MAE is less than 1.22 cm. For tree height extraction, the correlation coefficient (R^2) is above 0.90, RMSE ranges from 0.55 m to 1.63 m, and MAE is between 0.38 m and 0.85 m. For crown width extraction, the RMSE ranges from 0.91 m to 1.51 m, and MAE ranges from 0.78 m to 1.24 m. As the complexity of the sample plots increases, the extraction accuracy of all parameters decreases. 3) The fusion of multi-platform LiDAR data to obtain forest stand spatial structure can to some extent further replace field survey measurements. After performing the K-S test, there is no significant difference between the extracted values and the measured values for key forest stand spatial structure parameters (average angle scale, average neighborhood comparison) ($P > 0.05$). However, for the average crowding degree, there is a significant difference ($P < 0.05$). 4) The single-tree point cloud information extracted from the fused point cloud can be used for multi-variate distribution analysis of forest stand spatial structure. The research results show that the t-test results for the multi-variate distribution of forest stand spatial structure and the actual values do not show significant differences (P values > 0.05). The forest stand spatial structure obtained from the fused point cloud is as follows: the *Larix principis-rupprechtii Mayr* forest has a random distribution ($\overline{W} = 0.48$), moderate size differentiation ($\overline{U} = 0.50$), and average crowding degree ($\overline{C} = 0.75$); the *Picea wilsonii* forest has a random distribution ($\overline{W} = 0.48$), moderate size differentiation ($\overline{U} = 0.47$), and relatively dense state ($\overline{C} = 0.94$).

Author Contributions

Conceptualization, Hongke Hao and Ruiqiang Wang; investigation, Xuan Li, Ke Liu and Yan Li ; methodology, Hongke Hao and Ruiqiang Wang; resources, Hongke Hao; software, Ruiqiang Wang, Le Yang, Ke Liu, Tayeeba Tabussum Anni, Yan Li and Xuan Li; validation, Hongke Hao; formal analysis, Ruiqiang Wang and Hongke Hao; data curation, Hongke Hao and Ruiqiang Wang; writing—original draft preparation, Hongke Hao, Tayeeba Tabussum Anni, Ruiqiang Wang, Ke Liu, Yan Li, Bingqiang Bao and Xuan Li; visualization, Xuan Li and Bingqiang Bao. All authors have read and agreed to the published version of the manuscript.

Funding

This research received no external funding.

Institutional review board statement

Not applicable.

Informed consent statement

Not applicable.

Data availability statement

Not applicable.

Conflicts of interest

The authors declare no conflict of interest.

References

An H (2023) Study on the spatial structure of the broad-leaved Korean Pine forest. PhD Thesis, Beijing Forestry University, China.

Bai M, Zhang C, Chen Q, Wang J, Li H, Shi X, Tian X & Zhang Y (2021) Study on the extraction of individual tree height based on UAV visual spectrum remote sensing. Forest Resource Management 1: 164–172. doi:10.13466/j.cnki.lyzygl.2021.01.021.

Cao L, Liu H, Fu X, Zhang Z, Shen X & Ruan H (2019) Comparison of UAV LiDAR and digital aerial photogrammetry point clouds for estimating forest structural attributes in subtropical planted forests. Forests 10: 145. doi:10.3390/f10020145.

Chen S (2020) Extraction of individual tree and stand structure parameters based on RGB image of UAV in closed canopy mountainous Chinese Fir plantation. PhD Thesis, Zhejiang A&F University, China.

Chen Y (2017) Individual tree competition index and parameters estimation based on LiDAR data. PhD Thesis, Beijing Forestry University, China.

Dong L & Liu Z (2012) Visual management simulation for *Pinus sylvestris var. mongolica* plantation based on optimized spatial structure. Forest Science 48: 77–85. doi:10.11707/j.1001-7488.20121013.

Fu X (2010) Dynamic monitoring of plain plantation structure parameters based on airborne and UAV point cloud data . PhD Thesis, Nanjing Forestry University, China.

Guo Q, Li W, Yu H & Alvarez O (2010) Effects of topographic variability and LiDAR sampling density on several DEM interpolation methods. Photogrammetric Engineering & Remote Sensing 76: 701–712. doi:10.14358/PERS.76.6.701.

He J, Wang X, Wang K, Guo W, Liu L & Wang F (2021) Multivariate distribution of stand spatial structure parameters in poplar-birch secondary forest. Journal of Beijing Forestry University 43: 22–33. doi:10.12171/j.1000-1522.20200076.

Hu Y (2010) Structure-based spatial optimization management model for natural uneven-aged forest. PhD Thesis, Chinese Academy of Forestry, China.

Hu S, Liu J & Mao X (2017) Extraction and change of vegetation coverage of 2007–2010 in Northeast China. Journal of Northeast Forestry University 45: 45–50.

Hui G, Zhang L, Hu Y, Wang H & Zhang G (2016) Stand crowding degree and its applications. Journal of Beijing Forestry University 38: 1–6. doi:10.13332/j.1000-1522.20160107.

Li H, Lei J & Yang L (2016) Extraction of vegetation coverage and analysis of landscape pattern in rare earth mining area based on Landsat image. Transactions of the Chinese Society of Agricultural Engineering 32: 267–276. doi:10.11975/j.issn.1002-6819.2016.10.037.

Li Y (2013) The bivariate distribution of forest stand spatial structural parameters. PhD Thesis, Chinese Academy of Forestry, China.

Liu J, Wang H, He Y, Wang M, Li G, Yu D, Zhao P & Feng Z (2024) Application and challenges of UAV-based technology in precision forestry. Transactions of the Chinese Society of Agricultural Engineering 40: 1–11. doi:10.11975/j.issn.1002-6819.202312131.

Shi H, Wang X & Guo H (2008) Community structure and species diversity of *Larix principis-rupprechtii* plantation in Qinling Mountains. Anhui Agricultural Science Bulletin 15: 159–162, 204.

Shimizu K, Nishizono T, Kitahara F, Fukumoto K & Saito H (2022) Integrating terrestrial laser scanning and unmanned aerial vehicle photogrammetry to estimate individual tree attributes in managed coniferous forests in Japan. International Journal of Applied Earth Observation and Geoinformation 106: 102658. doi:10.1016/j.jag.2021.102658.

Sun M, Li Y, Chen Q & Cai G (2013) A progressive morphological filtering method for airborne LiDAR point cloud based on scan line. Opto-Electronic Engineering 40: 71–75. doi:10.3969/j.issn.1003-501X.2013.11.012.

Wan P, Zhang G, Wang H, Zhao Z, Hu Y, Zhang G, Hui G & Liu W (2019) Impacts of different forest management methods on the stand spatial structure of a natural Quercus aliena var. acuteserrata forest in Xiaolongshan, China. Ecological Informatics 50: 86–94. doi:10.1016/j.ecoinf.2019.01.007.

Wu X, Yang H, Lv Y, Wang Q & Sun Q (2019) Analysis of structure characteristics in *Picea asperata-Betula platyphylla* mixed forests. Journal of Beijing Forestry University 41: 64–72. doi:.10.13332/j.1000-1522.20180211.

Xie Y, Wang B, Yao Y, Yang L, Gao Y, Zhang Z & Lin L (2020) Quantification of vertical community structure of subtropical evergreen broad-leaved forest community using UAV-Lidar data. Acta Ecologica Sinica 40: 940–951. doi:10.5846/stxb201809282112.

Xu H (2018) Automatic estimation of forest plots parameter based on TLS and UAV image point clouds. PhD Thesis, Fuzhou University, China.

Xu T (2022) Study on single tree aboveground biomass estimation method based on ULS and TLS radar fusion data. PhD Thesis, Northeast Forestry University, China.

Yang M, Wang Y & Zhang X (2016) Study on the model for estimating forest volume of Chinese fir based on bi-source remote sensing data. Journal of Nanjing Forestry University (Natural Science) 40: 107–114. doi:10.3969/j.issn.1000-2006.2016.05.017.

Yu C, Wen X, Wang Q & Ye J (2024) Construction of a wood volume model based on branch attribute factors of ALS and TLS fusion data. Journal of Central South University of Forestry & Technology 3: 33–43. doi:10.14067/j.cnki.1673-923x.2024.03.004.

Zeng J (2019) Extraction of underforest topography and individual tree parameters of southern plantation by oblique photogrammetry. PhD Thesis, Beijing Forestry University, China.

Zhang G, Wang D, Liu W, Zhang C & Lv D (2014) Spatial parameters of *Larix principis-rupprechtii* with different diameter class at Huoditang Forest Region. Journal of Northwest Forestry University 29: 180–185. doi:10.3969/j.issn.1001-7461.2014.06.34.

Zhang G, Liu R, Hui G, Zhang G, Zhao Z & Hu Y (2019) *N*-variate distribution and its annotation on forest spatial structural parameters: a case study of *Quercus aliena* var. *acuteserrata* natural mixed forest in Xiaolong Mountains, Gansu

Province of northwestern China. Journal of Beijing Forestry University 41: 21–31. doi:10.13332/j.1000-1522.20180228.

Zhang W, Li D, Chen Y, Shao J, Shen A & Yan G (2018) Integration betweenTLS and UAVP hotogrammetry technology for Retrieving Tree Height. Journal of Beijing Normal University (Natural Science) 54: 764–771. doi:10.16360/j.cnki.jbnuns.2018.06.011.